AD-A168 966 A STUDY OF THE MECHANISM OF DYNAMIC DUCTILE FRACTURE OF 1/1
TWO-PHASE MATERIA..(U) WASHINGTON UNIV SEATTLE DEPT OF
MECHANICAL ENGINEERING M TAYA ET AL. 30 MAY 86
UNCLASSIFIED ARO-18325.7-EG DAAG29-82-K-0144 F/G 20/11 NL

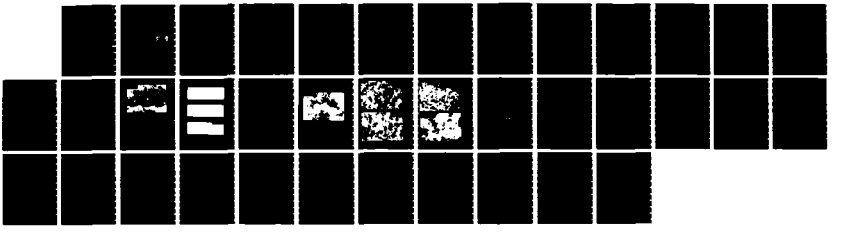

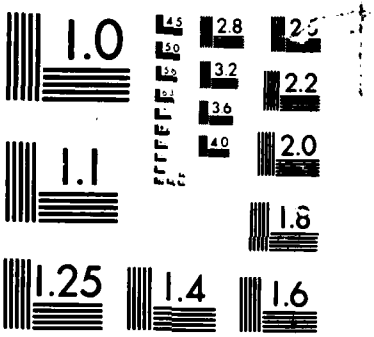
1.0
1.1
1.25
1.4
1.6
2.8
3.2
3.6
4.0
2.2
2.0
1.8

(2)

A STUDY OF THE MECHANISM OF DYNAMIC DUCTILE FRACTURE OF TWO-PHASE MATERIALS

FINAL REPORT

MINORU TAYA , UNIVERSITY OF WASHINGTON

IAN W. HALL AND H.S. YOON , UNIVERSITY OF DELAWARE

MAY 30 , 1986

U.S. ARMY RESEARCH OFFICE

DAAG29-82-K-0144

DEPARTMENT OF MECHANICAL ENGINEERING

UNIVERSITY OF WASHINGTON

SEATTLE, WA 98195

APPROVED FOR PUBLIC RELEASE;

DISTRIBUTION UNLIMITED.

THE VIEW, OPINIONS, AND/OR FINDINGS CONTAINED IN THIS REPORT ARE THOSE OF THE AUTHORS' AND SHOULD NOT BE CONTRUED AS AN OFFICIAL DEPARTMENT OF THE ARMY POSITION, OR DECISION, UNLESS SO DESIGNATED BY OTHER DOCUMENTATION.

UNCLASSIFIED
SECURITY CLASSIFICATION OF THIS PAGE (When Data Entered)

ADA 168 966

REPORT DOCUMENTATION PAGE		READ INSTRUCTIONS BEFORE COMPLETING FORM
1. REPORT NUMBER ARO 18325.7-EG	2. GOVT ACCESSION NO. N/A	3. RECIPIENT'S CATALOG NUMBER N/A
4. TITLE (and Subtitle) A Study of the Mechanism of Dynamic Ductile Fracture of Two-Phase Materials		5. TYPE OF REPORT & PERIOD COVERED Final Report, 1982-1985 6. PERFORMING ORG. REPORT NUMBER
7. AUTHOR(s) M. Taya, I.W. Hall and H.S. Yoon		8. CONTRACT OR GRANT NUMBER(s) DAAG29-82-K-0144
9. PERFORMING ORGANIZATION NAME AND ADDRESS University of Washington Department of Mechanical Engineering Seattle, WA 98195		10. PROGRAM ELEMENT, PROJECT, TASK AREA & WORK UNIT NUMBERS
11. CONTROLLING OFFICE NAME AND ADDRESS U. S. Army Research Office Post Office Box 12211 Research Triangle Park, NC 27709		12. REPORT DATE May 30, 1986 13. NUMBER OF PAGES 30
14. MONITORING AGENCY NAME & ADDRESS (if different from Controlling Office)		15. SECURITY CLASS. (of this report) Unclassified 15a. DECLASSIFICATION/DOWNGRADING SCHEDULE

16. DISTRIBUTION STATEMENT (of this Report)

Approved for public release; distribution unlimited.

17. DISTRIBUTION STATEMENT (of the abstract entered in Block 20, if different from Report)

NA

18. SUPPLEMENTARY NOTES

The view, opinions, and/or findings contained in this report are those of the author(s) and should not be construed as an official Department of the Army position, policy, or decision, unless so designated by other documentation.

19. KEY WORDS (Continue on reverse side if necessary and identify by block number)

Dynamic Ductile Fracture, Two-Phase Material, Composites, Metal Matrix Composites
High Strain-rate, Void Growth, Plate Impact Test, Split Hopkinson Bar Test

20. ABSTRACT (Continue on reverse side if necessary and identify by block number)

Dynamic ductile fracture of two-phase materials has been investigated ~~both~~ experimentally and analytically. This study consists of two stages. The first stage is a model study where an idealized two-phase material, single crystal Cu-SiO_2 was used to study the initiation and growth of voids, the dislocation morphology and the other microscopic behavior that took place in the as-impacted specimen. Some ~~of the~~ important findings are that voids were nucleated from only a fraction of secondary particles SiO_2, the larger strain has induced

DD FORM 1 JAN 73 1473 EDITION OF 1 NOV 65 IS OBSOLETE

UNCLASSIFIED
SECURITY CLASSIFICATION OF THIS PAGE (When Data Entered)

the higher void density, and the dislocation cell structures were formed with the average cell size being constant for the range of strain-rates investigated.

Then, analytical models were constructed with the aim of simulating the void growth in a two-phase material subjected to high strain-rate deformation, static void growth model and dynamic void growth model. A comparision between the experimental and analytical results of the void density has indicated that the static void growth model can predict the experimental results reasonably well for the smaller strain, but it fails to predict for the larger strain, while the dynamic void growth model can simulate the void growth well for the entire rage of strain and strain-rates.

The second stage of the study is to conduct a series of experiments on more realistic two-phase materials, Al-Si alloy and SiC_w or SiC_p/Al composite. In the experiment, the mode of the initiation and growth of voids was observed in the specimens that were impacted by Split Hopkinson bar test. The void density was also measured along the specimen axis and its values were compared with the analytical results by the static void growth model, resulting in a reasonably good agreement.

Foreword

Dynamic ductile fracture of a two-phase material has been investigated both experimentally and analytically. This study consists of two stages. The first stage is "a model study" where the idealized two-phase material, single crystal Cu-SiO_2 was used for both experimental and analytical studies. For the analytical study, the growth of voids was focused on, and two analytical models (static and dynamic void growth models) were constructed to simulate the simultaneous growth of voids which were nucleated from secondary particles. The experimental work was conducted by using plate impact test, which generated the distribution of voids in a Cu-SiO_2 plate, and the results of the void density f were compared with those predicted by the static and dynamic growth models. For smaller strain (or strain-rates), the static void growth model can predict the experimental results reasonably well, but it fails to predict for the larger strain-rates. While the dynamic void growth model can predict the experimental results reasonably well for the entire range of strain-rates.

TEM study conducted on the as-impacted Cu-SiO_2 specimens has revealed that dislocation cells were formed at higher strain-rates with the average cell diameter being 0.5 μm, and also that many microcrystallites ~10-50 nm in diameter were formed adjacent to the growing voids.

The second stage of this study is the experimental work on more realistic two-phase material systems, Al-Si alloy and SiC whisker/2124 Al composites which were subjected to uniaxial tension by split Hopkinson bar (SHB) with strain-rates 10^{-3}~10^{3}/sec. Then, the void density f was measured along the axis of the fractured specimen. The measured f was compared with the analytical results, resulting in a reasonably good agreement between them.

Table of Contents

I. List of Figures & Tables

Figure 12 Stress-strain curves of SiC_w/2124 Al at $\dot{e}$ = 600/sec with various volume fraction of SiC whisker.

Figure 13 Void density measured along the axis of the tensile SiC_w/2124 Al specimens with various volume fractions of SiC whisker.

Figure 14 Analytical model for the growth of voids.

Figure 15 The volume fraction of voids calculated by the static void growth model (f) vs the applied strain ($\dot{e}_{At}$) for the uniaxial strain mode.

Figure 16 The volume fraction of voids (f) calculated by the dynamic void growth model. The results for f_o = 0.005 and 0.0008 are plotted by solid and dashed curves, respectively and the experimental results by open symbols with the error arrow.

Table 1 Experimental results of the plate impact test on single crystal Cu-SiO_2.

Table 2 Comparison between the analytical results based on the static void growth model and experimental results.

II. Statement of the Problem

Most commercial metal alloys contain secondary particles (or fillers). If the matrix is ductile, the failure mode of the metal is ductile fracture, and its mechanism under quasi-static deformation has been well studied [1-13]. Based on these studies it was found that voids are nucleated at secondary particles and they grow continuously with the applied strain (stress), and ultimately coalesce, resulting in final fracture of the metal.

Unlike the case of quasi-static ductile fracture, only a limited amount of work has been carried out on the micro-mechanical aspects of dynamic ductile fracture of metals [14-17]. The previous experimental works on the dynamic ductile fracture of metals are focused on several metal systems, high purity aluminum and copper [14,15] and metal alloys [14,16] which are plate impacted. As to the analytical work on the dynamic ductile fracture, the mechanism of the initiation and growth of voids has been focused on [14,16]. The essence of the above analysis is based on the assumption that the matrix metal is linear viscous fluid [18]. On the other hand, Glennie [17] treated the void growth in a perfectly rigid plastic material by using the Hill's variational method [19] and modifying the static void growth model by Rice and Tracey [20].

The above brief review on the previous works on the dynamic ductile fracture of metals had led us to believe that the following subjects need to be focused on:

1. the mechanism of dynamic ductile fracture of an idealized two-phase material system (single crystal Cu-SiO_2).
2. the modeling of the dynamic void growth in a non-linear viscous metal.
3. the dislocation morphology in an as-impacted two-phase material.
4. the mechanism of dynamic ductile fracture of a new class of two-phase material including metal matrix composites (Al-Si alloy, SiC_p and SiC_w/Al composites).

In order to study the above subjects, we have conducted the following tasks:

Experimental Work

(i) Plate impact test on single crystal Cu-SiO_2 with several strain-rates.
(ii) Split Hopkinson bar (SHB) test on Al-Si alloy and SiC_w/Al composite.
(iii) Drop weight impact test on SiC_p/Al composite.
(iv) Metallographic study on the as-impacted specimen.

Analytical Work

(i) Construction of the static void growth model.
(ii) Construction of the dynamic void growth model.

III. Summary of the Most Important Findings

Both experimental and analytical works have led to a number of important findings, which will be given below.

1. Experimental Findings

Single crystal Cu-SiO_2 (Fig. 1) plates were plate impacted at various striking velocities, V_s = 110, 160 and 208 m/sec (see Fig.2 for the plate impact test apparatus). The impacted specimens were sectioned and examined by SEM (Fig.3), and the void density f across the plate thickness was measured (Fig. 4). The experimental results are summarized in Table 1. The as-impacted specimen was also examined by TEM. The SEM and TEM studies have revealed the following important findings [22]:

a. Void density f increases with the duration of the tensile stress wave (Δt, see Fig. 5 for its definition) and V_s. This observation is consistent with that by Seaman et al [14].

b. Only a fraction of secondary particle SiO_2 have nucleated voids (see Fig. 6), which is in marked contrast with the case of the quasi-static loading where virtually all the secondary particles (SiO_2) nucleate voids [21].

c. TEM study revealed the formation of dislocation cell structures in the as-impacted single crystal Cu-SiO_2 with the average cell diameter being constant (0.5 mμ) for the range of strain-rates investigated (10^4 ~ 10^5/sec) (see Fig. 7), and also that microcrystallites were formed near a large void (Fig. 8). The formation of microcrystallites is attributed to either dynamic recrystallization or recrystallization due to adiabatic heating.

In addition to the idealized two-phase material, we have also studied the dynamic ductile fracture of ordinary two-phase metals. Al-Si alloy and SiC whisker/2124 aluminum (SiC_w/Al) composite by subjecting them to uniaxial tension (Split Hopkinson Bar (SHB), see Fig. 9) at various high strain-rates up to 1500/sec. The dynamic stress-strain curves of these two-phase materials were obtained. Then the fractured specimens were sectioned along the specimen axis for the examination of the initiation and growth of voids by SEM. The above experimental study on the ordinary two-phase materials has led to the following findings:

d. Both Al-Si alloy and SiC_w/Al composite exhibited strong strain-rate sensitivity (see Fig. 10 for Al-Si alloy and Fig. 11 for SiC_w/Al with volume fraction of SiC whisker being 15%).

e. The higher the volume fraction of secondary filler (f_o), the larger the flow stress (Fig. 12) and also the higher the void density f (Fig. 13) become.

SiC particulate/6061 Al (SiCp/Al) composite was impacted by drop weight test and then subjected to three-point bending test to obtain the residual strength [29]. This drop weight test generates lower strain-rate, 10/sec. This study has yielded the following findings:

f. Voids were not observed in the as-impacted specimen.

q. The residual fracture energy of the as-impacted composite decreases with the increase in the impact energy and the rate of the reduction in the fracture energy becomes larger for smaller volume fraction of particles.

Table 1. Experimental Results [22]

	Symbols	Case 1	Case 2	Case 3
Striking velocity of projectile (m/s)	V_s	110.	160.	208.
Hugoniot elastic limit (GPa)	σ_e	0.164	0.164	0.164
Elastic particle velocity (mm/μs)	u_e	0.00415	0.00415	0.00415
Elastic stress wave velocity (mm/μs)	U_e	4.46	4.46	4.46
Plastic particle velocity (mm/μs)	u_p	0.055	0.080	0.104
Plastic stress wave velocity (mm/μs)	U_p	4.0018	4.0393	4.0747
Initial density of Cu (mm/μs)	ρ_o	8.93	8.93	8.93
Density of Cu behind the plastic shock front	ρ_1	9.01	9.06	9.10
Duration (μs)	Δt	0.186	0.190	0.195
Strain-rate (10^4/s)	$\dot{e}_A$	5.5	8.0	10.4
Applied strain (10^{-2})	$\dot{e}_A \Delta t$	1.023	1.52	2.028

2. Analytical Findings

In order to predict the void density observed in the as-plate impacted Cu-SiO_2 and also the as-SHB tested ordinary two-phase materials, we have constructed two analytical models, static void growth model [11,13,24] and dynamic void growth model [22,26]. The semi-detailed statement of the static and dynamic void growth model is given in Appendices. It was assumed in our model that voids of the same size will grow simultaneously under applied strain, $\dot{e}_A t$ where $\dot{e}_A$ and t are applied strain-rate and time, respectively (Fig. 14). In our models, we focus on a representative void (the solid circle in Fig. 14) which is surrounded by a mixture of voids and incompressible matrix metal and have calculated the

growth of the representative void. Thus, the surrounding media becomes compressible as far as the volume fraction of voids (f) > 0. In this respect, the interaction between growing voids can be taken into account, whereas the other models cannot account for this interaction since they focus on a single void surrounded by incompressible matrix. The analytical study has led to the following findings.

a. A comparison between the experimental results of the peak values of f (Fig. 4) and the analytical results by our static void growth model [24] revealed that the static void growth model can predict the void density f reasonably well for smaller $\dot{e}_{At}$, but it fails for larger $\dot{e}_{At}$ (Fig. 15). f_o in Fig. 15 denotes the initial volume fraction of voids and should be less than or equal to 0.005 which is the volume fraction of the secondary particle SiO_2. f_o was found to be about 0.0008 [22].

b. Our dynamic void growth model [26] can account for the interaction between growing voids, material non-linearity ($1 \leq n \leq \infty$) and inertia effect. Besides, this model can yield the existing solutions as special cases, i.e., the solutions of the dynamic void growth by Poritsky for linear viscous metal [18], and by Gennie for perfectly rigid plastic material ($n = \infty$) [17], and those of the static void growth by Budiansky et al [10]. The analytical results by our dynamic void growth model can predict the experimental results of the peak value of f in the as-plate impacted Cu-SiO_2 well (see Fig. 16). It can be concluded from Fig. 16 that the matrix metal (Cu) exhibits a weak non-linearity, n=1.5 (see the definition of n in Appendix B).

c. Another important finding in the dynamic void growth by our model [26] is that the non-dimensional parameter y_o defined by strain-rate, initial radius of the void and material parameters (see the definition of y_o in Appendix B) play a dominant role on the dynamic void growth. Namely, when y_o is large, the inertia effect is to reduce the growth rate at the initial stage of void growth. If y_o is small, the dynamic void growth can be approximated by the static growth model. The material non-linearity has a strong effect on the

void growth for smaller y_o (quasi static growth), but a weak effect on the void growth for larger y_o (dynamic growth).

d. The void density measured in the as-SHB tested ordinary two-phase material was compared with that predicted by the static void growth model, resulting in a reasonably good agreement though the analytical prediciton fails to explain the trend of the increase in f as $\dot{e}$ increases (see Table 2) [30]. Then the dynamic void growth model was applied to this case, leading to the better agreement between the experimental and analytical results. In using the dynamic model, the ratio of the mean stress to the effective stress was properly estimated by use using the results by Needleman [27].

Table 2 Comparison between the experimental and analytical results [30]

strain-rate, $\dot{e}$	Void density measured		Void density predicted by the static void growth model	
Location from the fracture section	2 mm	0 mm	2 mm	0 mm
493	0.0013	0.005	0.002	0.012
1,109	0.005	0.025	0.002	0.012
1,530	0.009	0.035	0.0021	0.013

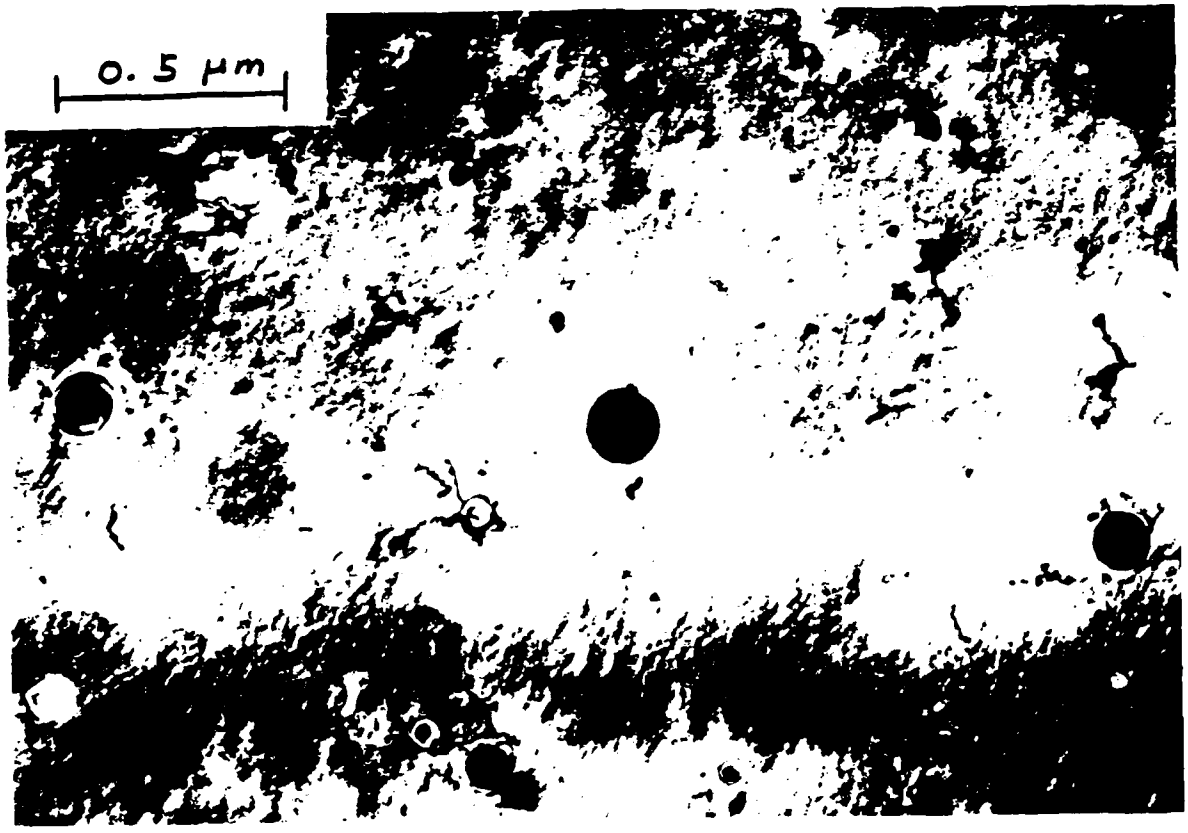
0.5 μm

Fig. 1

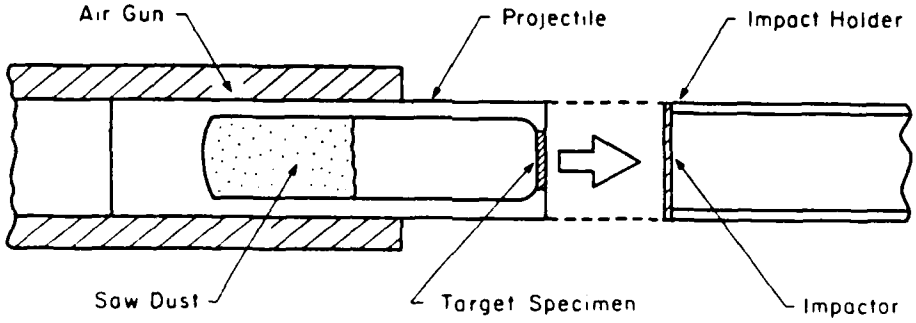
Air Gun
Projectile
Impact Holder
Saw Dust
Target Specimen
Impactor

Fig. 2

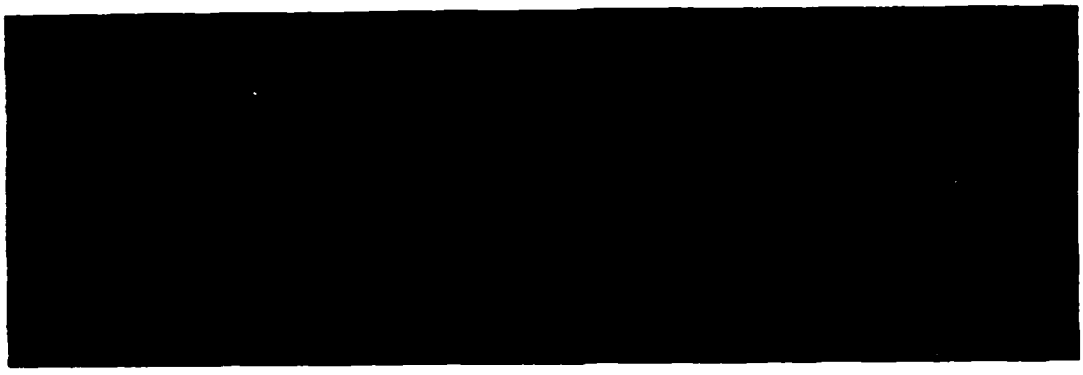

(a)

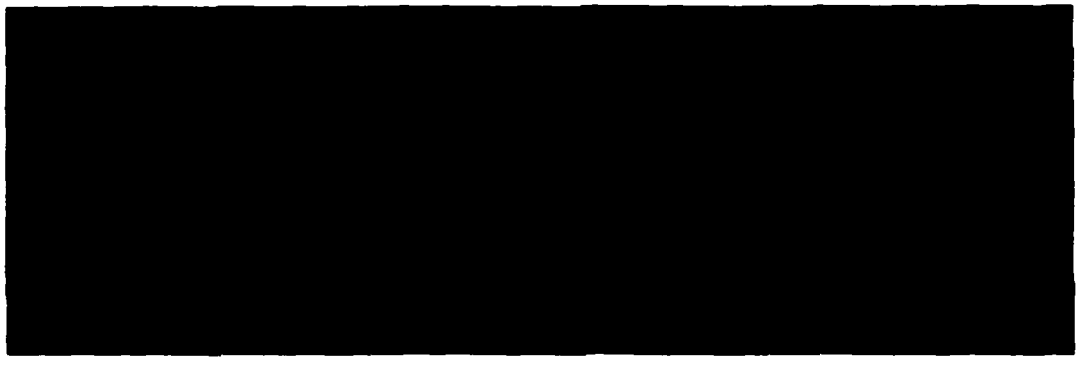

(b)

(c)

Fig. 3

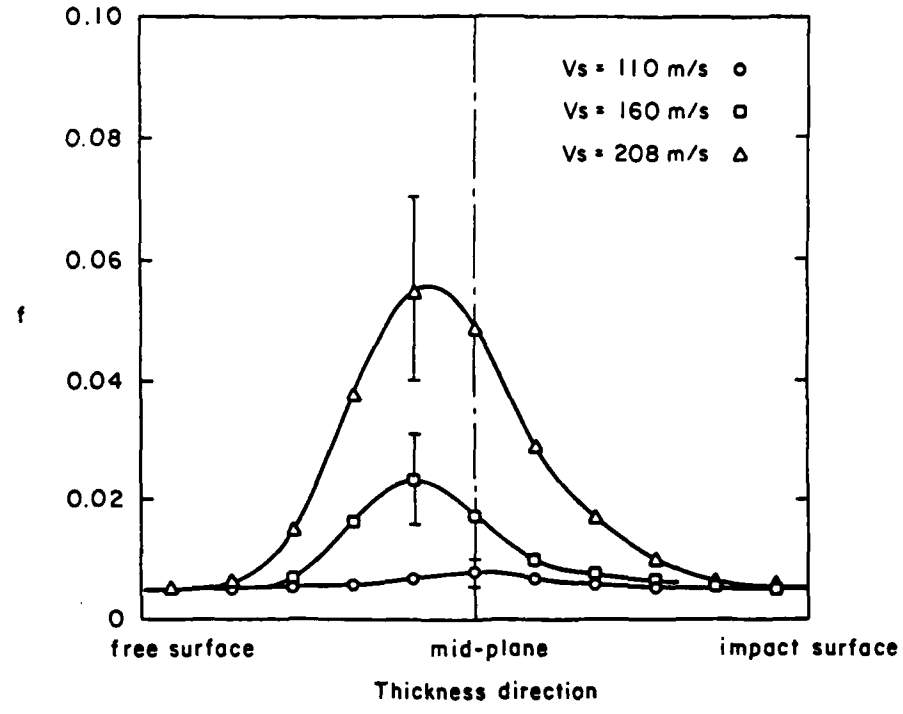
0.10
0.08
0.06
0.04
0.02
0
f
Vs = 110 m/s o
Vs = 160 m/s □
Vs = 208 m/s △
free surface
mid-plane
impact surface
Thickness direction

Fig. 4

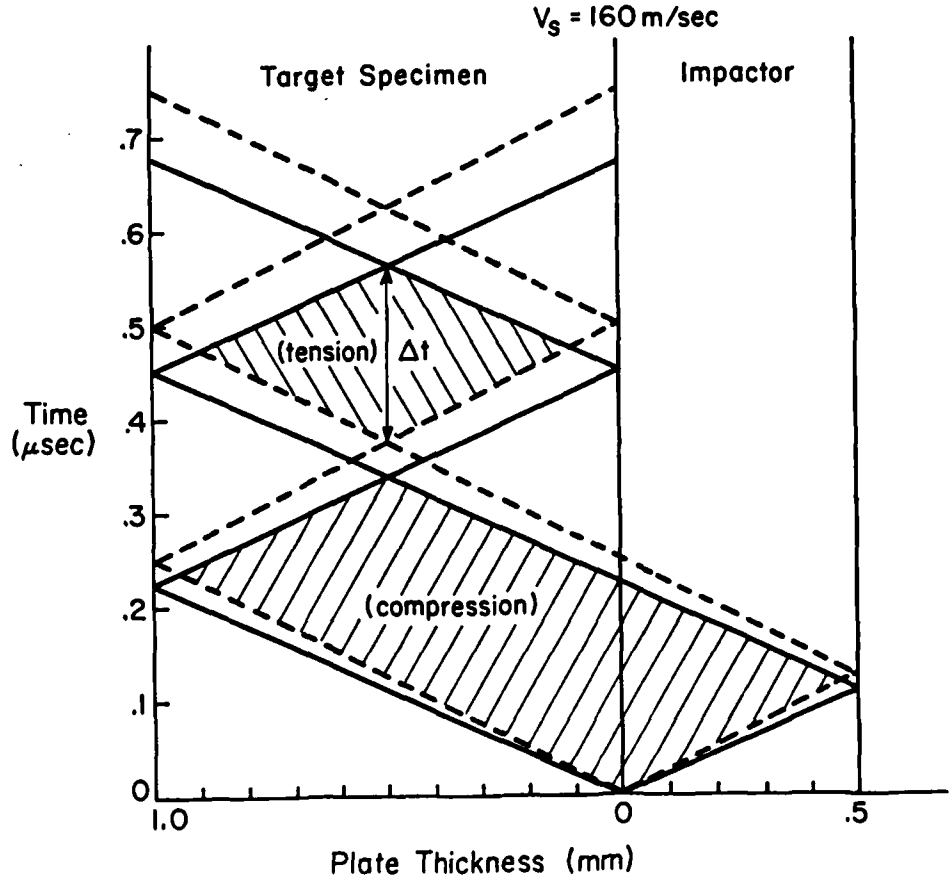
Vs = 160 m/sec
Target Specimen
Impactor
.7
.6
.5
.4
.3
.2
.1
0
Time (μsec)
(tension)
Δt
(compression)
1.0
0
.5
Plate Thickness (mm)

Fig. 5

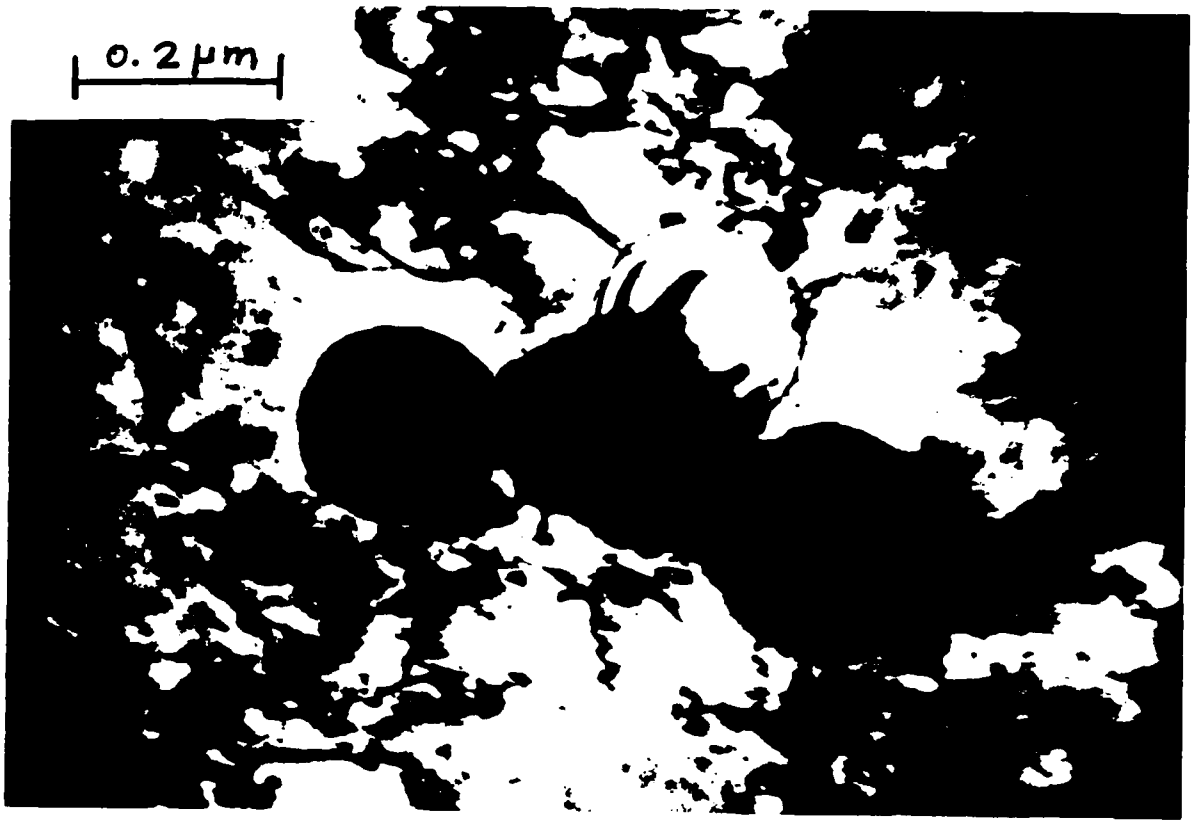

Fig. 6

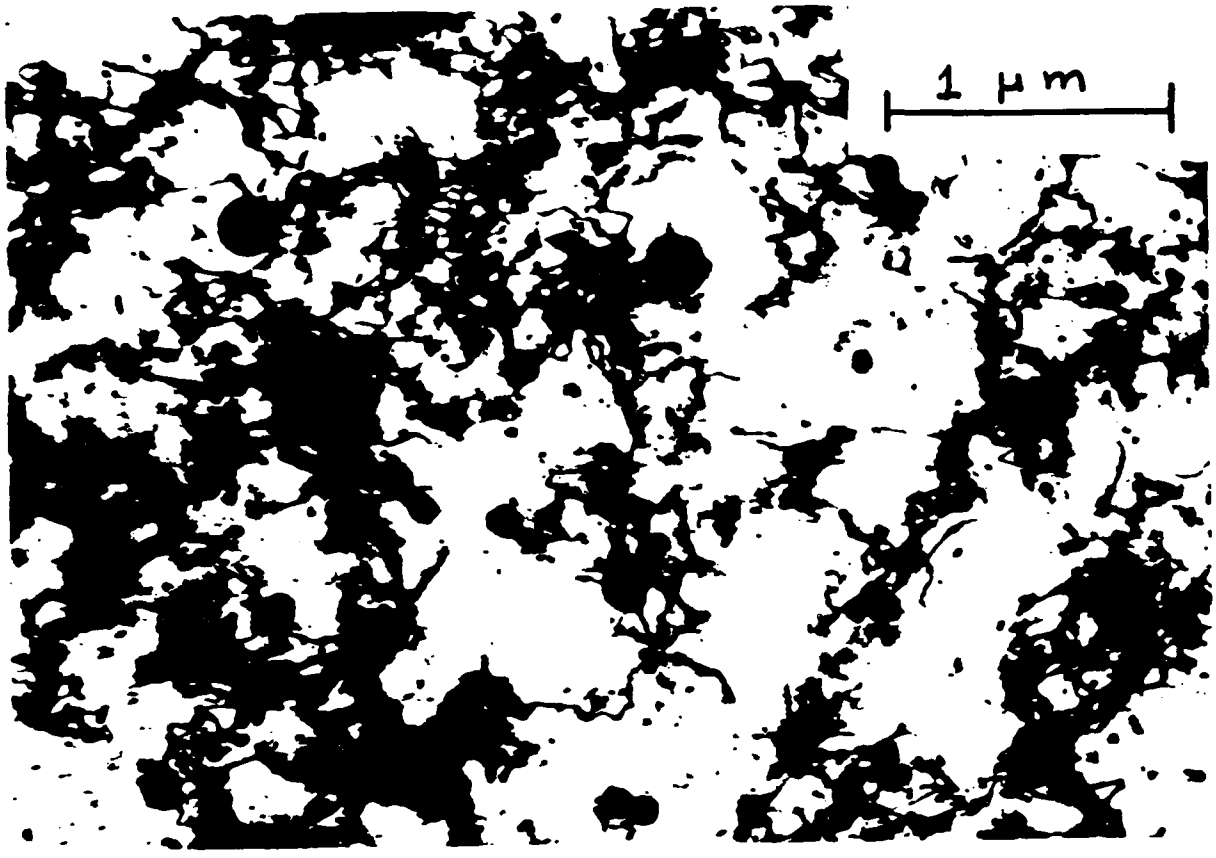

Fig. 7(a)

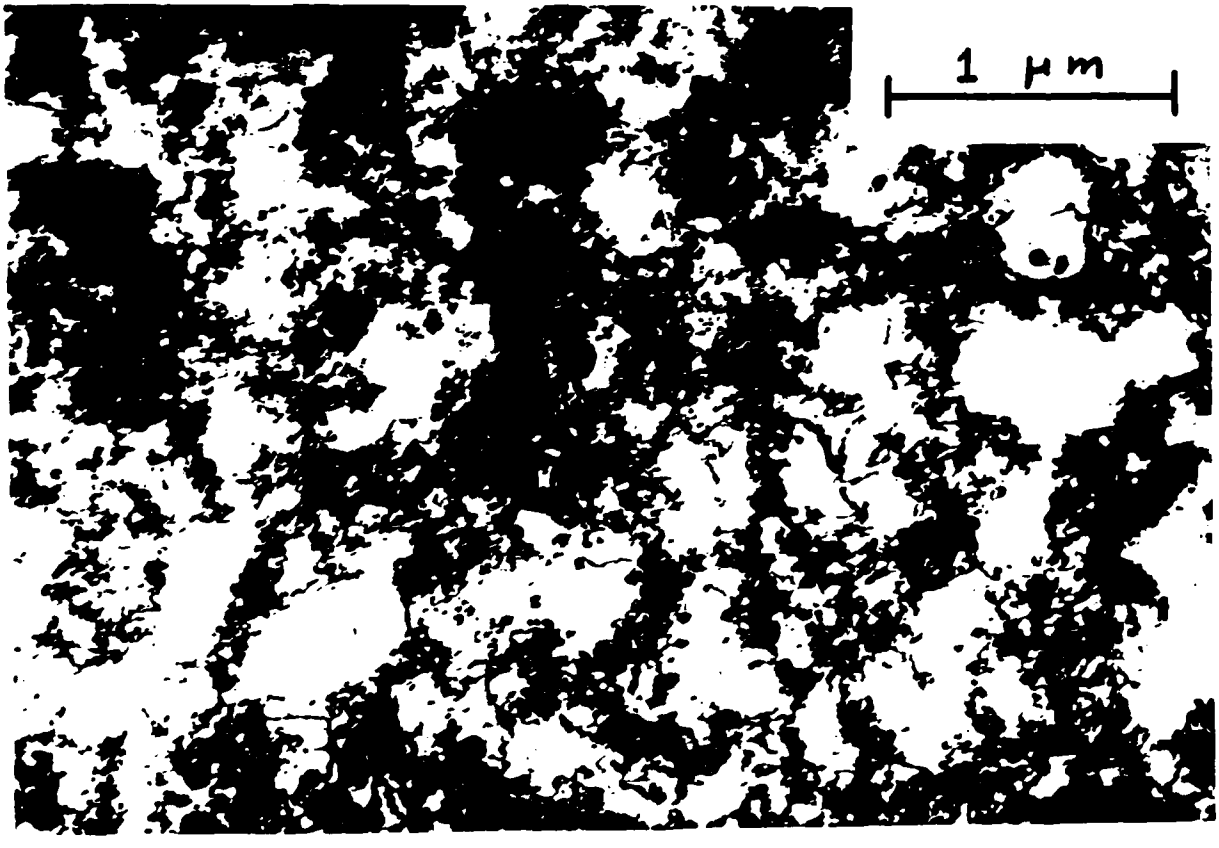

Fig. 7(b)

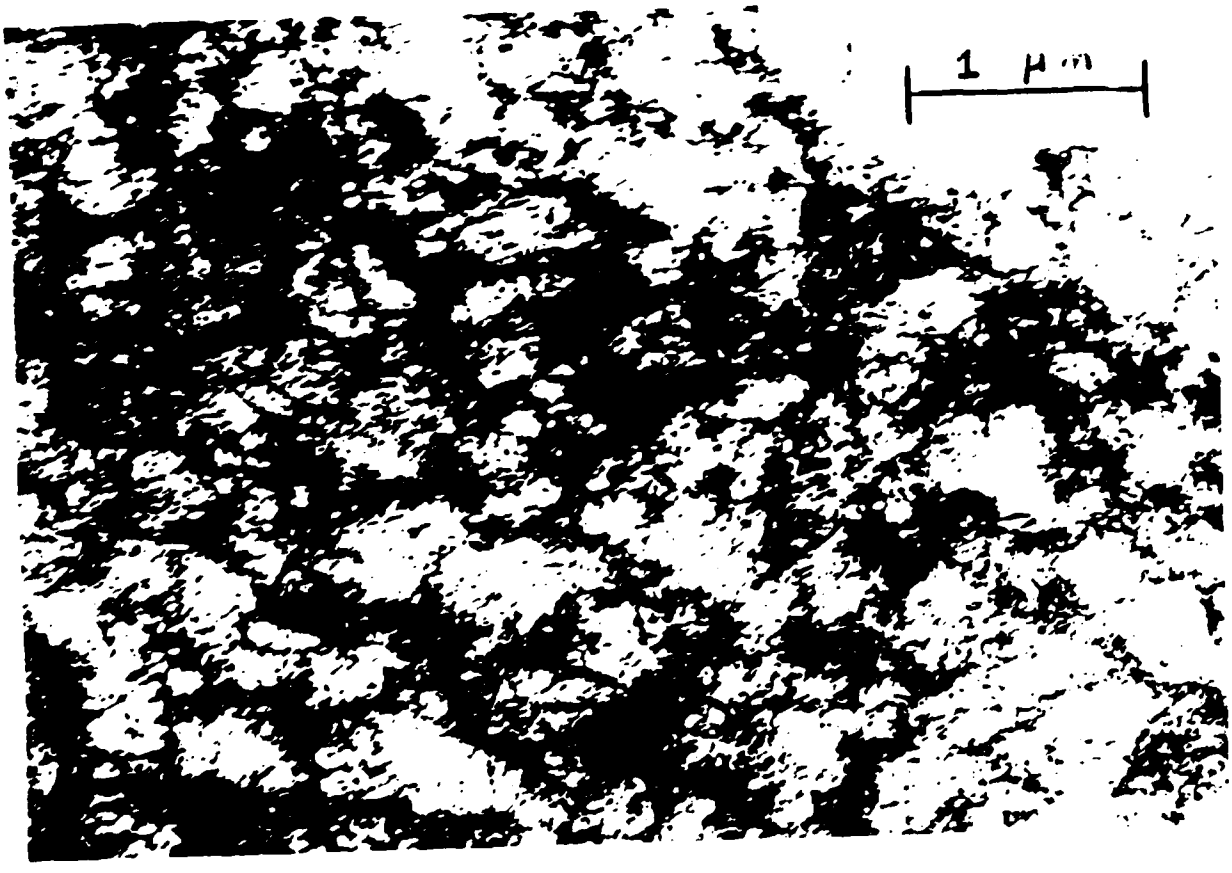

Fig. 7(c)

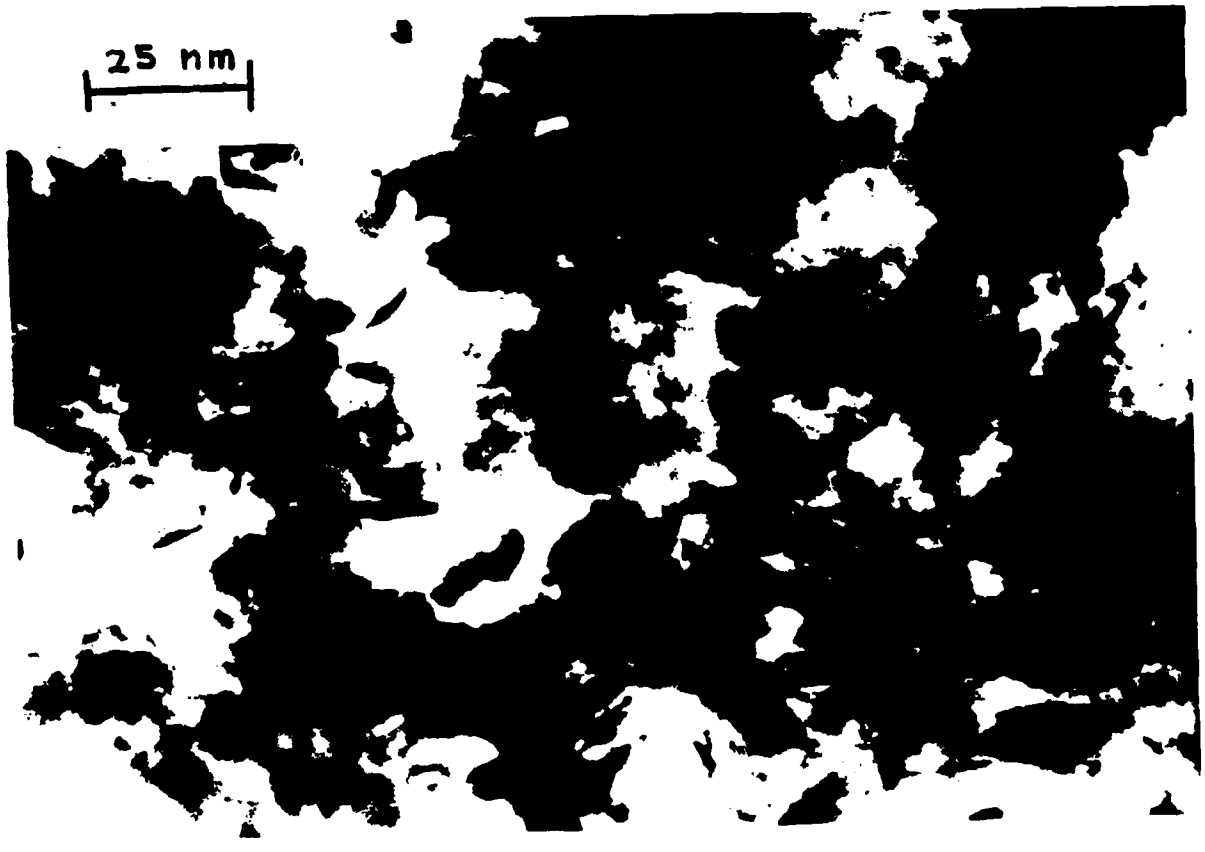

Fig. 8

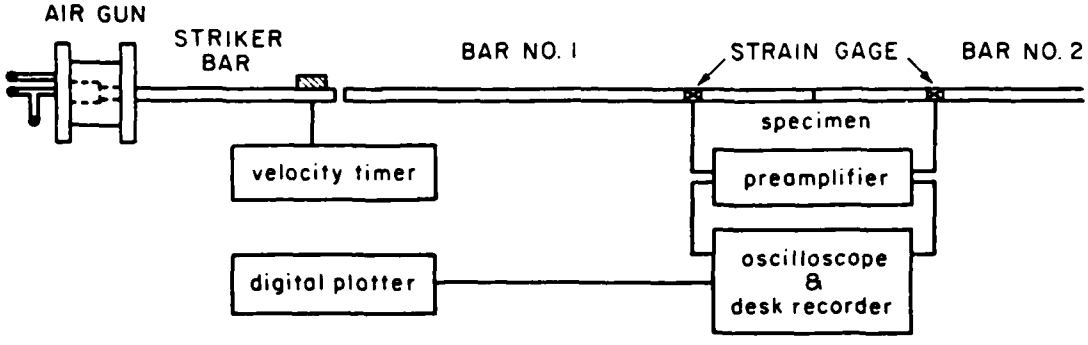
AIR GUN
STRIKER BAR
BAR NO. 1
STRAIN GAGE
BAR NO. 2
specimen
velocity timer
preamplifier
digital plotter
oscilloscope & desk recorder

(a)

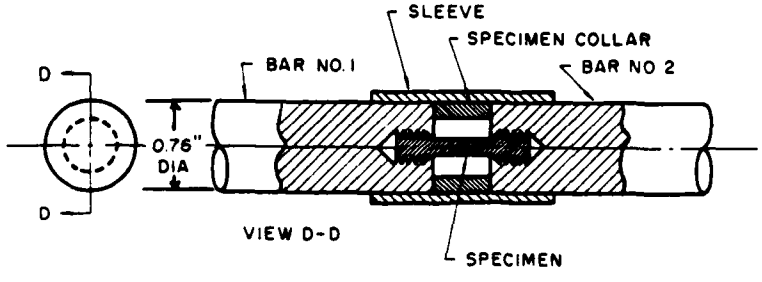
SLEEVE
SPECIMEN COLLAR
BAR NO. 1
BAR NO 2
D
D
0.76" DIA
VIEW D-D
SPECIMEN

(b)

Fig. 9

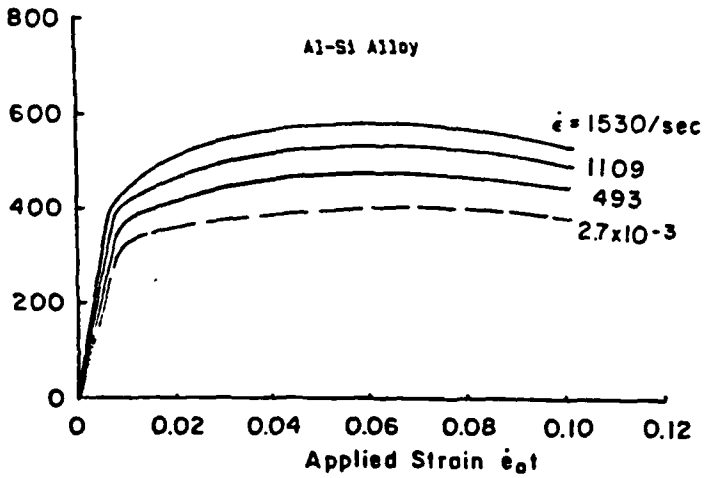

Fig. 10

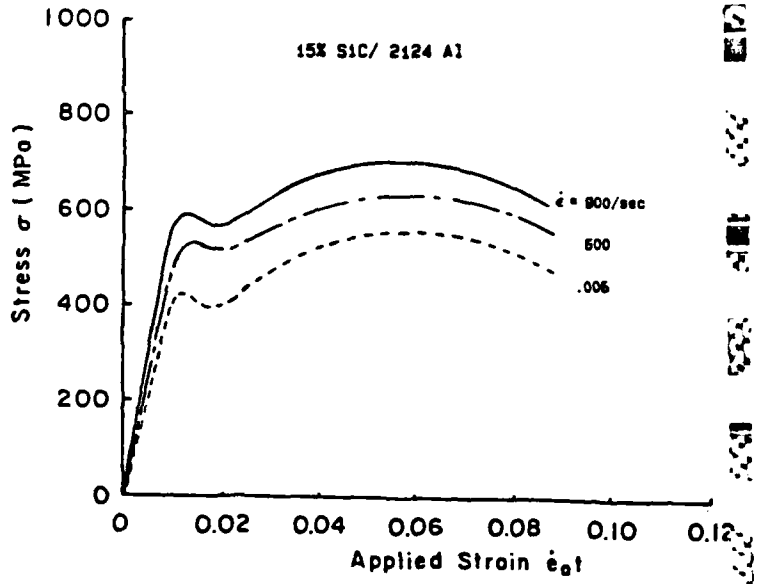

Fig. 11

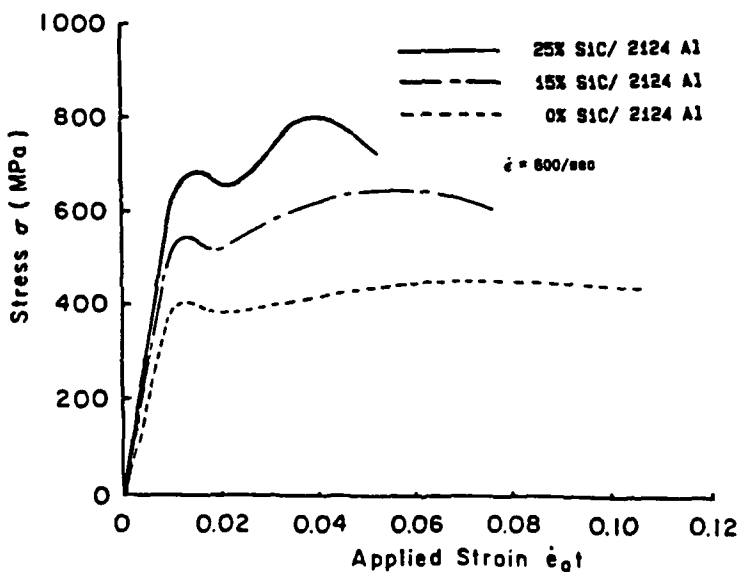

Fig. 12

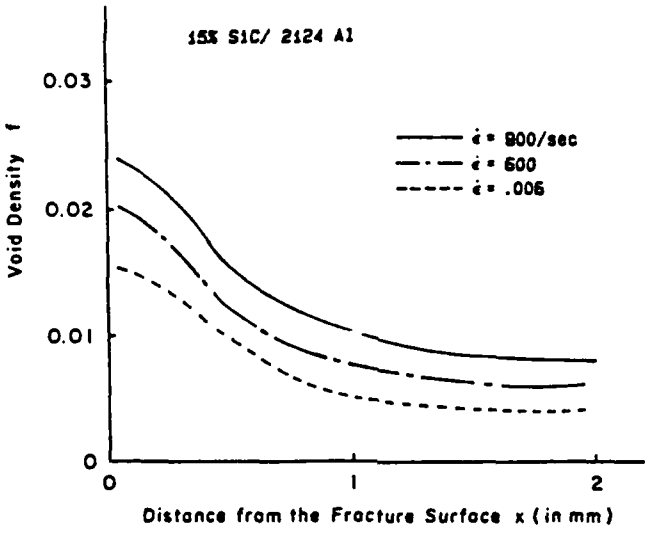
15% SiC/ 2124 Al
0.03
0.02
0.01
0
Void Density f
$\dot{\epsilon}$ = 900/sec
$\dot{\epsilon}$ = 600
$\dot{\epsilon}$ = .006
0
1
2
Distance from the Fracture Surface x (in mm)

Fig. 13

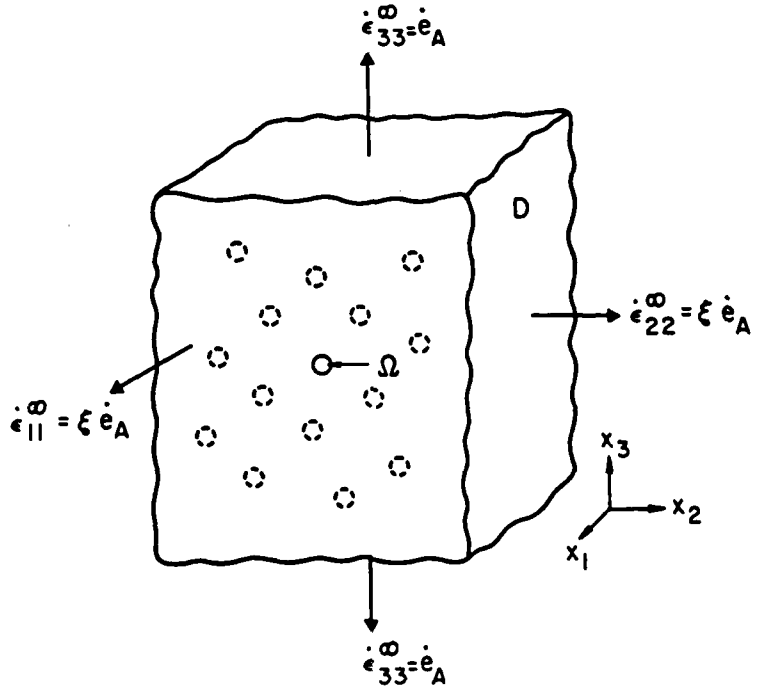
$\dot{\epsilon}^{\infty}_{33}=\dot{e}_A$
D
$\dot{\epsilon}^{\infty}_{22}=\xi\,\dot{e}_A$
Ω
$\dot{\epsilon}^{\infty}_{11}=\xi\,\dot{e}_A$
x_3
x_2
x_1
$\dot{\epsilon}^{\infty}_{33}=\dot{e}_A$

Fig. 14

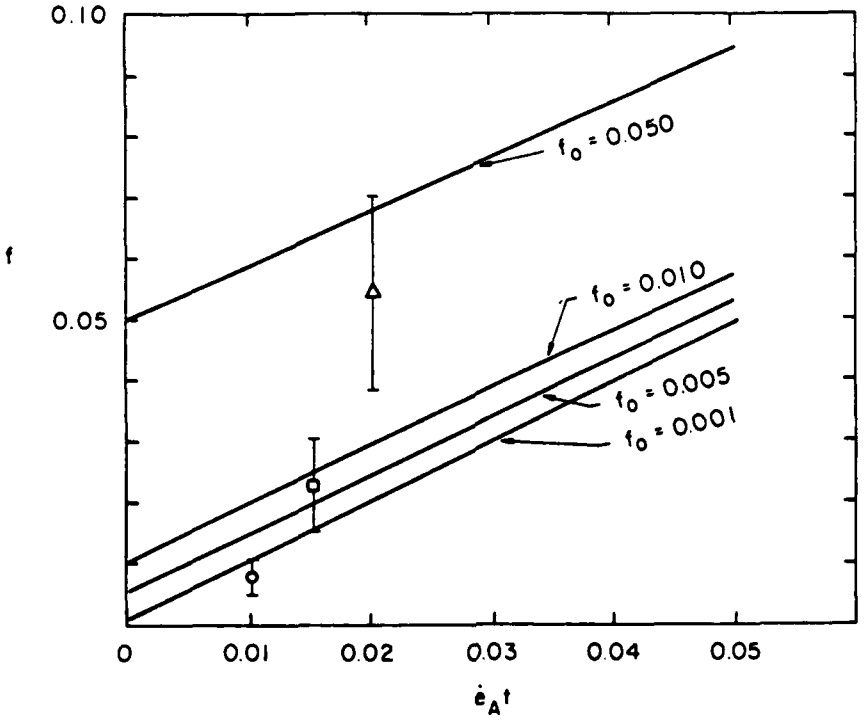
0.10
0.05
f
0
0.01
0.02
0.03
0.04
0.05
$\dot{e}_A t$
$f_0 = 0.050$
$f_0 = 0.010$
$f_0 = 0.005$
$f_0 = 0.001$

Fig. 15

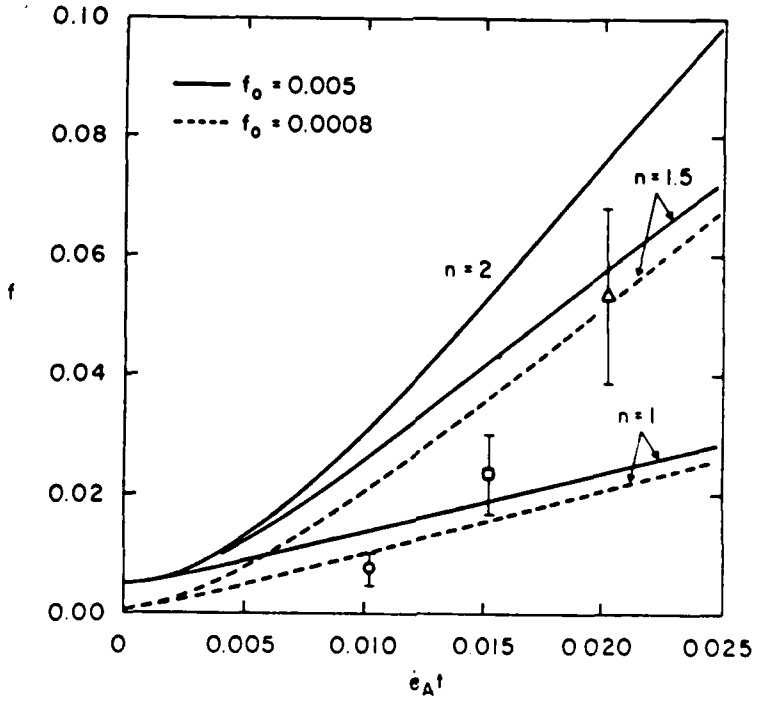
0.10
0.08
0.06
0.04
0.02
0.00
f
0
0.005
0.010
0.015
0.020
0.025
$\dot{e}_A t$
$f_0 = 0.005$
$f_0 = 0.0008$
n = 2
n = 1.5
n = 1

Fig. 16

IV. List of Publications

1. Publications

M. Taya, I.W. Hall and H.S. Yoon, "Mechanism of Void Growth in Single Crystal Cu-SiO_2 Under High Strain-Rate Deformation," Proceedings of the Fourth Risø International Symposium on Metallurgy and Materials Science: Deformation of Multi-Phase and Particle Containing Materials, September, 1983. Risø, Denmark, supplement pp. 1-10.

H.S. Yoon and M. Taya, "Prediction of the Void Growth at its early Stage in a Viscous Two-Phase Material," International Journal of Engineering Science, Vol. 22, No. 8/10 (1984), pp. 1035-1040.

M. Taya, I.W. Hall, H,S. Yoon and V.S. Pritchard, "Fracture Mode of Single Crystal Cu-SiO_2 Subjected to Unidirectional High Strain-Rate Impact," the Abstracts of the 20th SES Meeting, 1983, University of Delaware, edited by M. Taya and F.A. Kulacki.

M. Taya, I.W. Hall, H.S. Yoon and D.S. Pritchard, "Void Growth in a Two-Phase Material Subjected to High Strain-Rate Impact," in Mechanical Properties at High Rates of Strain 1984, edited by J. Harding, Institute of Physics Conf. Ser. No. 70, pp. 269-276.

W.G. Patterson and M. Taya, "Residual Strength of Preimpacted SiC/6061 Aluminum Composites," in Advances in Aerospace Sciences and Engineering, edited by U. Yuceoglu and R. Hesser, ASME AD-08, Bound Volume, (1984), pp. 49-54.

M. Taya, I.W. Hall and H.S. Yoon, "Void Growth in a Single Crystal Cu-SiO_2 Plate at High Strain-Rate," Acta Metallurgica, Vol. 33, No. 12, (1985), pp. 2143-2153.

M. Taya, I.W. Hall and H.S. Yoon, "Dynamic Void Growth in a Two-Phase Material under Uniaxial Tension," Proceedings of the IUTAM Symposium on Macro- and Micro-Mechanics of High Velocity Deformation and Fracture, Tokyo, 1985, edited by K. Kawata, Springer Verlag, in press.

H.S. Yoon and M. Taya, "Dynamic Void Growth in a Non-Linear Viscous Solid," submitted for publication in Mechanics of Materials.

V. List of Participating Scientific Personnel

1. M. Taya, Associate Professor
   Mechanical Engineering
   University of Washington

2. I.W. Hall, Assistant Professor
   Mechanical and Aerospace Engineering
   University of Delaware

3. H.S. Yoon, Ph.D. Candidate
   Mr. Yoon earned M.S. in Mechanical and Aerospace Engineering in 1984.

4. W.G. Patterson, Ph.D. Candidate

VI. References

1. K.E. Puttick, Phil. Mag. Ser. 4, 964 (1959).
2. F.A., McClintock, J. App. Mech. 35, 363 (1968).
3. C.A. Berg, Fourth U.S. Natn. Cong. Appl. Mech., ASME, 885 (1962).
4. J. Gurland, Acta Metall. 20, 735 (1972).
5. L.M. Brown and J.D. Embury, Proc. 3rd Inst. Conf. Strength of Metals and Alloys, Cambridge, p. 164, (1973).
6. T.B. Cox and J.R. Low, Jr., Metall. Trans, 5, 1457 (1974).
7. L.M. Brown and W.M. Stobbs, Phil. Mag. 34, 351 (1976).
8. A.S. Argon and J. Im, Metall. Trans. A6, 839 (1976).

9. S.H. Goods and L.M. Brown, Actal metall. 27, 1 (1979).
10. B. Budiansky, J.W. Hutchinson and S. Slutsky, Mechanics of Solids: The Rodney Hill 60th Ann. Vol. (edited by H.G. Hopkins and M.J. Sewell), p. 13 (1981).
11. M. Taya and E.D. Seidel, Int. J. Engr Sci. 19, 1083 (1981).
12. G. LeRoy, J.D. Embury, G. Edwards and M.F. Ashby, Acta Metall. 29, 1509 (1981).
13. M. Taya and W.G. Patterson, J. Mater. Sci. 17, 115 (1982).
14. L. Seaman, T.W. Barber, Jr and D.R. Curran, U.S. Air Force Weapon Lab. Rep. AFWL-TR-71-156.
15. J.W. Edington, Phil Mag. 19, 1189 (1969).
16. G.L. Moss and L. Seaman, Mech. of Mater. 1,87 (1982).
17. E.B. Glennie, J. Mech. Phys. Solids 20, 415 (1972).
18. H. Poritsky, Proc. First U.S. Natn. Cong. Appl. Mech. ASME, p. 813 (1951).
19. R. Hill, J. Mech. Phys. Solids 11, 305 (1963).
20 J.M. Rice and D.M. Tracey, J. Mech. Phys. Solids 17, 201 (1969).
21. I.G. Palmer and G.C. Smith, Oxide Dispersion Strengthening, Metall. Soc. AIME Conf. Vol. 47, p. 253 (1966).
22. M. Taya, I.W. Hall and H.S. Yoon, Acta Metall. 33, 2143 (1985).
23. M. Taya, I.W. Hall, H.S. Yoon and D.S. Pritchard, Inst. Phys. onf. Ser. 70, 269 (1984).
24. H.S. Yoon and M. Taya, Int. J. Engr Sci. 22, 1035 (1984).
25. J.D. Eshelby, proc. R. Soc. Lond. A241, 376 (1957).
26. H.S. Yoon and M. Taya, submitted for publication.
27. A. Needleman, J. Appl. Mech. 39, 964 (1972).
28. J.M. Duva and J.W. Hutchinson, Mech. of Mater., 3, 41 (1984).
29. W.G. Patterson and M. Taya, in Advances in Aerospace Sciences and Engineering, edited by U. Yuceoglu and R. Hesser, ASME-08, Bound Volume, 49 (1984).
30. M. Taya, I.W. Hall and H.S. Yoon, Proc. IUTAM Symposium on Macro- and Micro-Mechanics of High Velocity Deformation and Fracture, edited by K. Kawata, Springer Verlag, 1986, in press.

VII. Appendices

Appendix A: Static Void Growth Model

It is assumed in our theoretical model that the effect of inertia can be neglected at the early stage of void growth, the voids grow simultaneously and the matrix is incompressible viscous material at high strain-rate: $\sigma = 2\mu_o \dot{e}$ where σ is the stress, $\dot{e}$ is the strain-rate and μ_o is the viscosity. Here the two-phase material consists of a ductile matrix obeying $\sigma = 2\mu_o \dot{e}$ and spherical particles which nucleate spherical voids. After voids are nucleated, they grow under the applied strain-rate which is assumed to be constant. Then the composite that consists of the incompressible matrix and voids becomes compressible due to the existence of the voids. In order to solve the problem of void growth, we focus on a representative void that is surrounded by the composite media subjected to $\dot{e}_A$ along the x_3-axis as shown in Fig. 14. The coefficient ξ in Fig. 14 denotes either the case of uniaxial tension ($\xi = -\nu$), or uniaxial strain ($\xi = 0$) or that of triaxial stress ($\xi = 1$). The composite has two constants, the effective viscosity (μ) and the effective expansion coefficient (κ), and they are given by [11].

$$\mu = \mu_o \{1 + \frac{5f}{3(1-f)}\} \tag{1}$$

$$\kappa = \frac{4\mu_o}{3} \cdot \frac{(1-f)}{f} \tag{2}$$

where μ_o is the viscosity of the incompressible matrix material and f is the volume fraction of voids. For later convenience, the domain of the representative void is denoted by Ω and that of the whole composite by D, then that of the surrounding media becomes D-Ω.

Applying Eshelby's equivalent inclusion method [25], we have in Ω

$$\lambda\delta_{ij}(\dot{e}^{o}_{kk} + \dot{e}_{kk} - \dot{e}^{*}_{kk}) + 2\mu(\dot{e}^{o}_{ij} + \dot{e}_{ij} - \dot{e}^{*}_{ij}) = 0 \tag{3}$$

where $\lambda = \kappa - 2\mu/3$, μ and κ are defined by eqs. (1) and (2), δ_{ij} is the Kronecker's delta, the super dots denote the material time derivative, $\dot{e}^{o}_{ij}$ is the applied strain-rate, $\dot{e}^{*}_{ij}$ is the eigenstrain-rate that has some value in Ω, but vanishes in $D - \Omega$, and $\dot{e}_{ij}$ is the disturbance of the strain-rate due to the existence of Ω and is related to $\dot{e}^{*}_{k\ell}$ as [25]

$$\dot{e}_{ij} = S_{ijk\ell}\dot{e}^{*}_{k\ell} \tag{4}$$

where $S_{ijk\ell}$ is the Eshelby's tensor and its explicit expressions for Ω being sphere and prolate ellipsoid are given in Appendix C. By setting $i = j$ in eq. (3) and noting that $3\lambda + 2\mu = \kappa \neq 0$ due to voids, we obtain

$$\dot{e}^{o}_{kk} + \dot{e}_{kk} - \dot{e}^{*}_{kk} = 0 \tag{5}$$

where the repeated index is to be summed over 1, 2 and 3. Also by setting $i = j = 3$ in eq. (3), we have

$$2S_{3311}\dot{e}^{*}_{11} + (S_{3333} - 1)\dot{e}^{*}_{33} = -\dot{e}_{A} \tag{6}$$

where we have used the fact that the system of Fig. 14 gives rise to transverse isotropy and hence only independent components are those with $ij = 11$ (or 22) and 33. The shape of Ω will become sphere for $\xi = 1$ and prolate ellipsoid for $\xi = -\nu$ and 0 under the applied strain-rate $\dot{e}^{o}_{ij}$. Let us denote the axes of the major and minor of the prolate ellipsoid by c and a. Then the growth rate of the axes are given by

$$\frac{\dot{a}}{a} = \dot{e}^{o}_{11} = \dot{e}_{11} \tag{7}$$

$$\frac{\dot{c}}{c} = \dot{e}^{o}_{33} + \dot{e}_{33} \tag{8}$$

After having solved for $\dot{e}^{*}_{11}$ and $\dot{e}^{*}_{33}$ in eqs. (5) and (6), then using eqs. (4), (7) and (8), we arrive at for triaxial stress ($\xi = 1$),

$$\frac{\dot{a}}{a} = \frac{\dot{c}}{c} = \frac{\dot{e}_{A}}{\{1 - S_{1111} - S_{1122}\}} \tag{9}$$

for uniaxial strain ($\xi = 0$),

$$\frac{\dot{a}}{a} = \left[\frac{S_{1133}(S_{1111} + S_{1122}) + (1 - S_{1111} - S_{1122})S_{1133}}{(1 - S_{1111} - S_{1122})(1 - S_{3333}) - 2S_{1133}S_{3311}} \right] \dot{e}_A \tag{10}$$

$$\frac{\dot{c}}{c} = \left[1 + \frac{2S_{1133}S_{3311} + (1 - S_{1111} - S_{1122})S_{3333}}{(1 - S_{1111} - S_{1122})(1 - S_{3333}) - 2S_{1133}S_{3311}} \right] \dot{e}_A \tag{11}$$

and for uniaxial stress ($\xi = -\nu$),

$$\frac{\dot{a}}{a} = \left[-\nu + \frac{\{S_{1133} - \nu(1-S_{3333})\}(S_{1111}+S_{1122}) + (1-S_{1111}-S_{1122}-2\nu S_{3311})S_{1133}}{\{(1-S_{1111}-S_{1122})(1-S_{3333}) - 2S_{1133}S_{3311}\}} \right] \dot{e}_A \tag{12}$$

$$\frac{\dot{c}}{c} = \left[1 + \frac{2S_{3311}\{S_{1133} - \nu(1-S_{3333})\} + \{1-S_{1111}-S_{1122}-2\nu S_{3311}\}S_{3333}}{\{(1-S_{1111}-S_{1122})(1-S_{3333}) - 2S_{1133}S_{3311}\}} \right] \dot{e}_A \tag{13}$$

Once a and c are computed at current time, then the current volume fraction of void, f, can be obtained from

$$f = \frac{a^2 c}{a_o^2 c_o} \tag{14}$$

In eqs. (12) and (13), ν is defined by

$$\nu = \frac{2\eta - 1}{4\eta + 1} \tag{15}$$

$$\eta = \frac{(1 - f)}{f\{1 + \frac{5f}{3(1-f)}\}}$$

Dynamic Void Growth Model

Here, we use the same theoretical model as that for the static void growth (Fig. 14) except that the non-linearity of the material is introduced in the present model.

The infinite body D is subjected to the applied strain-rate at far field, $\dot{\varepsilon}^{\infty}_{11} = \dot{\varepsilon}^{\infty}_{22} = \xi\dot{e}_A$ and $\dot{\varepsilon}^{\infty}_{33} = \dot{e}_A$ as shown in Fig. 14. The strain-rate field is axi-symmetric with respect to the x_3-axis and the corresponding stresses are also axi-symmetric with respect to x_3-axis and can be obtained explicitly in terms of applied strain-rate if the constitutive equation of the material is known.

The non-linear material considered is isotropic and compressible with power law dependence of the strain-rate on stress. Under simple tension, the total strain-rate ($\dot{\varepsilon}$) is related to the stress (σ) by

$$\dot{\varepsilon} = \dot{\varepsilon}_o(\frac{\sigma}{\sigma_o})^n \tag{1}$$

where σ_0 and $\dot{\varepsilon}_0$ are the reference stress and strain-rate, respectively. The rate hardening exponent n ranges from 1 to ∞. For the multiaxial case, the corresponding deviatoric stress (s_{ij}) can be related to the deviatoric strain-rate ($\dot{e}_{ij}$) as

$$s_{ij} = \frac{2\sigma_o}{3\dot{\varepsilon}_o}(\frac{\sigma_e}{\sigma_o})^{1-n}\dot{e}_{ij} \tag{2}$$

where σ_e is the effective stress defined by $\sigma_e = (\frac{3}{2}s_{ij}s_{ij})^{1/2}$ [28], and the repeated indices are to be summed (this rule will be used throughout this paper). Eq. (2) is derived from the assumption that the deviatoric stress is linearly related to the deviatoric strain-rate and the effective deviator is strain-rate (Γ) is related to the effective stress (σ_e) as

$$\Gamma = \dot{\varepsilon}_o(\frac{\sigma_e}{\sigma_o})^n \tag{3}$$

where $\Gamma = (\frac{2}{3}\dot{e}_{ij}\dot{e}_{ij})^{1/2}$ Noting that for the linear viscous material the viscosity is obtained as a slope of σ-ε curve and s_{ij} in eq. (2) becomes equal to $2\mu\dot{e}_{ij}$, we can set μ as

$$\mu = \frac{\sigma_o}{3\dot{\varepsilon}_o} \tag{4}$$

Here σ_o is assumed to be related to the volume fraction of the voids f in accordance with μ in eq. (1) of Appendix A. Then the total stress can be written by

$$\sigma_{ij} = -p\delta_{ij} - 2\mu\,(\frac{\sigma_e}{\sigma_o})^{1-n}\,\dot{e}_{ij} \tag{5}$$

where p is the hydrostatic pressure and σ_e/σ_o is given by

$$\frac{\sigma_e}{\sigma_o} = (\frac{3\mu\Gamma}{\sigma_o})^{1/n} \tag{6}$$

The extreme cases of these materials are a linear viscous material with n = 1 and a rigid/plastic material with $n \to \infty$.

Let us introduce a representative void Ω of radius R in the origin of the compressible body (Fig. 14) and apply the variational principle proposed by Hill [19] and also used by Glennie [17] to the problem of dynamic void growth in a non-linear compressible viscous material D. Following Glennie, the approximate velocity field $\tilde{u}_j$ can be the solution of the problem provided that

$$\int_{D-\Omega}\{(\sigma_{ij}-\sigma^{\infty}_{ij})\frac{\partial\omega_j}{\partial x_i} + \omega_j(\rho\frac{D\tilde{u}_j}{Dt} - g_j - \frac{\partial\sigma^{\infty}_{ij}}{\partial x_i})\}dV = -\int_{\Omega}\sigma^{\infty}_{ij}\omega_j n_i dS \tag{7}$$

for any velocity field w_j, where σ_{ij} and σ^{∞}_{ij} are the stress field corresponding to the assumed velocity field and the stress field at the outer boundary, respectively, ρ is the density of the matrix and D/Dt is the material time derivative.

In general, the velocity can be approximated as

$$\tilde{u}_i = \dot{\varepsilon}^{\infty}_{ij} x_j + \tilde{Du}^{D}_i + \tilde{Eu}^{E}_i \tag{8}$$

where $\tilde{u}_i{}^D$ represents a spherically symmetric expansion, while $\tilde{u}_i{}^E$ denotes the shape distorsion of the void. Both fields should vanish at large distance from the void. However, noting that the effect of the shape change can be neglected under high stress triaxiality [10,20], we consider only the dilational growth field $\tilde{u}_i{}^D$ and use the same velocity field as those used by Rice and Tracey [20] under the assumption that the disturbance velocity field is limited in the small vicinity of void and from the fact that the pure matrix is incompressible. Thus we have

$$\tilde{u}_i = \dot{\varepsilon}^{\infty}_{ij} x_j + \tilde{Du}^{D}_i \tag{9}$$

where

$$\tilde{u}^D_i = \dot{\varepsilon}^{\infty}_e \left(\frac{R}{r}\right)^3 x_i \ , \ \dot{\varepsilon}^{\infty}_e = \left(\frac{2}{3}\dot{\varepsilon}^{\infty}_{ij}\dot{\varepsilon}^{\infty}_{ij}\right)^{1/2} \ , \ r = (x_i x_i)^{1/2}$$

and R is the radius of a representative void. The normalizing field w_j in eq. (7) is defined as

$$\omega_j = \frac{x_j}{r^3} \tag{10}$$

It is noted here that $\tilde{u}_i{}^D$ and w_j die out as the distance r from the origin increases. After some manipulation (see the details in [26]), we arrive at the following growth equation

$$\frac{\dot{R}}{R} = \frac{(1-\xi)\dot{e}_A}{3}\left[\frac{3}{2n}\left\{\frac{\sigma^{\infty}_m}{\sigma_{e^{\infty}}} - \frac{\rho}{\sigma_{e^{\infty}}}\left(R\ddot{R}+\frac{3}{2}\dot{R}^2\right) - \frac{(1+2\xi)}{3}R\dot{R}\dot{e}_A - \frac{(1+2\xi^2)}{6}R^2\dot{e}_A{}^2\right\}\right.$$

$$\left. + \frac{(n-1)(n+0.432)}{n^2}\right]^n \tag{11}$$

where the stress ratio $(\sigma^{\infty}_m/\sigma^{\infty}_e)$ for various boundary conditions must be given. The effective stress at far field $\sigma_e{}^{\infty}$ is given by

$$\frac{\sigma_e^{\infty}}{\sigma_o} = \left\{\frac{2\mu(1-\xi)\dot{e}_A}{\sigma_o}\right\}^{1/n} \tag{12}$$

However, the mean stress σ_m^{∞} at remote boundary cannot be given explicitly except for the linear viscous material (n = 1) which is given by

$$\sigma_m^{\infty} = \kappa\, \dot{\varepsilon}_{kk}^{\infty}, \quad \dot{\varepsilon}_{kk}^{\infty} = (1 + 2\xi)\dot{e}_A \tag{13}$$

Hence, the stress ratio α for n = 1 is set to

$$\alpha = \frac{\sigma_m^{\infty}}{\sigma_e^{\infty}} = \left(\frac{\kappa}{2\mu}\right)\frac{(1 + 2\xi)}{(1 - \xi)} = \frac{(1 + \nu)}{3(1 - 2\nu)}\,\frac{(1 + 2\xi)}{(1 - \xi)} \tag{14}$$

and it is assumed that eq. (14) holds for the non-linear material in order to have the same condition on α. The stress ratio α in eq. (14) is dependent not only on the mode parameter ξ but also on the Poisson's ratio ν, thereby α is a function of the volume fraction of voids f.

Next let us consider three kinds of straining mode, i.e., $\xi = 0$, $-\nu$ and 1. However, when the initial volume fraction of voids (f_o) is zero, the surrounding matrix becomes strictly incompressible. Then the stress ratio α given by eq. (14) becomes infinite, which means infinite void growth except for the case of $\xi = -\nu$. When $\xi = -\nu$ (uniaxial tension mode), α becomes finite (1/3). Especially, if $\xi = -\nu = -1/2$, $\dot{\varepsilon}_{kk} = 0$ as seen in eq. (13) and our growth equation can give rise to the existing solutions in which the surrounding matrix is assumed to be incompressible. Under these conditions ($\xi = -\nu = -1/2$, $f_o = 0$), the effective strain-rate $\dot{\varepsilon}_e$ is equal to $\dot{e}_A$ and eq. (11) is reduced to

$$\frac{\dot{R}}{R} = \frac{\dot{\varepsilon}_e^{\infty}}{2}\left[\frac{3}{2n}\left\{\left(\frac{\sigma_m^{\infty}}{\sigma_e^{\infty}}\right) - \frac{\rho}{\sigma_e^{\infty}}\left(R\ddot{R} + \frac{3}{2}\dot{R}^2 - \frac{R^2}{4}(\dot{\varepsilon}_e^{\infty})^2\right)\right\} + \frac{(n-1)(n+0.432)}{n^2}\right]^n \tag{15}$$

By setting n = 1 and using eq. (3.6), we can simplify eq. (3.28) as

$$\frac{\dot{R}}{R} = \frac{1}{4\mu}\left[\sigma_m^{\infty} - \rho\left(R\ddot{R} + \frac{3}{2}\dot{R}^2 - \frac{R^2}{4}(\dot{\varepsilon}_e^{\infty})^2\right)\right] \tag{16}$$

which is the same as the classical solution [18] derived from the Bernoulli equation except that the last term inside the bracket is added and pressure difference is replaced by σ_m^∞ here. For n being infinity, we have from eq. (15)

$$\frac{\dot{R}}{R} = \lim_{n\to\infty} \frac{\dot{\varepsilon}_e^\infty}{2}\left[\frac{3}{2n}\left\{\left(\frac{\sigma_m^\infty}{\sigma_e^\infty}\right) - \frac{\rho}{\sigma_{e\infty}}\left(R\ddot{R}+\frac{3}{2}\dot{R}^2 - \frac{R^2}{4}(\dot{\varepsilon}_e^\infty)^2\right)\right\} + \frac{(n-1)(n+0.432)}{n^2}\right]^n$$

$$= 0.283\dot{\varepsilon}_e^\infty \exp\left[\frac{3}{2}\left(\frac{\sigma_m^\infty}{\sigma_e^\infty}\right) - \frac{\rho}{\sigma_e^\infty}\left(R\ddot{R} + \frac{3}{2}\dot{R}^2 - \frac{R^2}{4}(\dot{\varepsilon}_e^\infty)^2\right)\right] \qquad (17)$$

which coincides with the Glennie's solution [17] by using $\sigma_e^\infty = \sqrt{3}\,\tau_o$. Furthermore, if we neglect the inertia term, eq. (15) is reduced to

$$\frac{\dot{R}}{R} = \frac{\dot{\varepsilon}_e^\infty}{2}\left[\frac{3}{2n}\left(\frac{\sigma_m^\infty}{\sigma_e^\infty}\right) + \frac{(n-1)(n+0.432)}{n^2}\right]^n \qquad (18)$$

which was obtained by Budiansky et al for the quasi-static void growth in a non-linear viscous material [10]. Thus, the dynamic void growth equation derived here can include the existing solutions for special cases, in which the material is assumed to be incompressible.

For the case of uniaxial strain mode ($\xi = 0$), eq. (11) is reduced to

$$\frac{\dot{R}}{R} = \frac{\dot{e}_A}{3}\left[\frac{3}{2n}\left\{\alpha - \frac{\rho}{\sigma_e^\infty}\left(R\ddot{R} + \frac{3}{2}\dot{R}^2 - \frac{1}{3}R\dot{R}\dot{e}_A - \frac{1}{6}R^2\dot{e}_A^2\right)\right\} + \frac{(n-1)(n+0.432)}{n^2}\right]^n \qquad (19)$$

where $\alpha = (1+\nu)/3(1-2\nu)$. Then we can obtain the volume fraction of voids by solving eq. (19) by the Runge-Kutta method. Since we will simulate the void growth by the present model in a ductile metal impacted by flyer test that gives rise to the state of uniaxial strain (Taya et. al [22]), we focus only on the numerical results for the uniaxial strain mode ($\xi = 0$).

Appendix C

The Eshelby's tensors $S_{ijk\ell}$ are given in [28]. We present them in a more convenient form below. The suffices ijkℓ in the Eshelby's tensors are consistent with the coordiante systems (Fig.14).

1. When Ω is a sphere

$$S_{1111} = S_{2222} = S_{3333} = \frac{(7 - 5\nu)}{15(1 - \nu)}$$

$$S_{1122} = S_{2233} = S_{3311} = \frac{-(1 - 5\nu)}{15(1 - \nu)}$$

$$S_{1212} = S_{2323} = S_{3131} = \frac{(4 - 5\nu)}{15(1 - \nu)}$$

2. When Ω is prolate spheroid along x_3-axis

$$S_{1111} = S_{2222} = \frac{1}{8(1 - \nu)}\left[3\left\{1 + \frac{1}{\beta^2 - 1}\right\} + \left\{1 - 2\nu - \frac{9}{4(\beta^2 - 1)}\right\}I_o\right]$$

$$S_{3333} = 1 + \frac{1}{(1 - \nu)}\frac{\beta^2}{(\beta^2 - 1)} - \frac{1}{4(1 - \nu)}\left\{1 - 2\nu + \frac{3\beta^2}{(\beta^2 - 1)}\right\}I_o$$

$$S_{1122} = S_{2211} = \frac{1}{8(1 - \nu)}\left[1 + \frac{1}{\beta^2 - 1} - \left\{\frac{3}{4}\frac{1}{(\beta^2 - 1)} + 1 - 2\nu\right\}I_o\right]$$

$$S_{1133} = S_{2233} = \frac{1}{2(1 - \nu)}\left[-\frac{\beta^2}{\beta^2 - 1} + \frac{1}{4}\left\{\frac{3\beta^2}{\beta^2 - 1} - (1 - 2\nu)\right\}I_o\right]$$

$$S_{3311} = S_{3322} = \frac{1}{2(1 - \nu)}\left[-\left\{1 - 2\nu + \frac{1}{\beta^2 - 1}\right\} + \frac{1}{4}\left\{\frac{3}{\beta^2 - 1} + 2(1 - 2\nu)\right\}I_o\right]$$

where $\beta = \frac{c}{a}$

$$I_o = \frac{2\beta}{(\beta^2 - 1)^{3/2}}\left\{\beta(\beta^2 - 1)^{1/2} - \cosh^{-1}\beta\right\}$$

END

DTIC

8-86